Single mode to dual mode switch through a THz reconfigurable metamaterial

Zhang, Wu; Zhang, Meng; Yan, Zongkai; Zhao, Xin; Cheng, Jianping; Liu, Ai Qun

2017

Zhang, W., Zhang, M., Yan, Z., Zhao, X., Cheng, J., & Liu, A. Q. (2017). Single mode to dual mode switch through a THz reconfigurable metamaterial. Applied Physics Letters, 111(24), 241106-. doi:10.1063/1.5008984

https://hdl.handle.net/10356/103245

https://doi.org/10.1063/1.5008984

Single mode to dual mode switch through a THz reconfigurable metamaterial

Wu Zhang,[1,2,a),b)] Meng Zhang,[1,3,a)] Zongkai Yan,[1,4] Xin Zhao,[5] Jianping Cheng,[3] and Ai Qun Liu[2]

[1]*Harvard John A. Paulson School of Engineering and Applied Sciences, Harvard University, Cambridge, Massachusetts 02138, USA*
[2]*School of Electrical and Electronic Engineering, Nanyang Technological University, Singapore 639798, Singapore*
[3]*School of Energy Science and Engineering, Harbin Institute of Technology, Harbin 150001, China*
[4]*School of Energy Science and Engineering, University of Electronic Science and Technology of China, Chengdu 611731, China*
[5]*College of Physical Science and Technology, Sichuan University, Chengdu 610064, China*

(Received 11 October 2017; accepted 4 December 2017; published online 14 December 2017)

Metamaterials interact with incident electromagnetic waves through their consisting subwavelength metamolecules. In this paper, we reported a reconfigurable metamaterial which tunes its THz response experimentally from a single mode resonance at 2.99 THz to a dual mode resonance at 2.94 THz and 2.99 THz. The reconfiguration is realized through a micromachined actuator, and the tunability is achieved by breaking the symmetry of the metamolecule. An abrupt change in the transmission is experimentally observed when the gap between two metallic structures is closed, and a decrease in transmission from 40% to 5% at 2.94 THz is obtained. Such a tunable metamaterial promises widespread applications in optical switches, filters, and THz detectors. *Published by AIP Publishing.*
https://doi.org/10.1063/1.5008984

Metamaterials are artificial materials consisting of engineered subwavelength structures namely metamolecules.[1–3] Metamolecules are usually designed in special structures such as split ring resonators,[4,5] fishnets,[6,7] and paired slabs[8] to induce desired interactions with incident electromagnetic (EM) waves. The interaction leads to optical properties rarely found in natural materials, such as negative refraction,[9,10] extraordinary transmission,[11–13] and abnormal refraction.[14,15] Numerous applications are accordingly realized including invisible cloaking,[16–18] superlens,[19] perfect absorption,[20–22] and flat lens focusing.[23,24]

The ever-increasing demand on the optical information transmission and processing inspires various active optical devices like optical switches,[25] phase shifters,[26] and light modulators.[27] Metamaterials, which control EM waves with high flexibility, have gained high research interest for active manipulation on the amplitude,[28,29] phase,[30] and polarization[31] of light in either single bands or multi-bands. Many works focus on tuning the consisting material properties of metamaterials through different excitation methods. For example, electrical bias,[32,33] optical pumping,[29,34] and thermal effect[35] are applied to manipulate the refractive index of the consisting material. These methods usually simply shift the resonant frequency of the metamaterial. A more flexible method is to reconfigure metamaterials. Different techniques are developed such as deforming soft material based substrates,[36,37] controlling cantilevers in metamolecules,[38] or shifting metamolecules through a micromachine.[39–41] The reconfiguration changes metamolecule shapes and tailors the coupling between different segments in the metamolecule. As a result, the metamaterial's response to EM waves is manipulated significantly in real time.

In this paper, we demonstrated the tuning of a single mode resonance to a dual mode resonance in the THz regime through a reconfigurable metamaterial (RMM). The tuning is realized by breaking the symmetry of the metamolecule structure. The consisted metallic strips in the metamolecule are driven by a micromachined actuator, and the metallic strip movement effectively manipulates the coupling condition in the metamaterial. Moreover, by closing the gap between two metallic strips, an abrupt resonance switch is obtained. The promising tunability of the RMM has potential applications such as high sensitive THz detectors, optical switches, and switchable filters.

The designed RMM consists of a planar array of metamolecules with three metallic strips as shown in Fig. 1(a). One strip is along the y-axis and located at the center of the metamolecule. The other two are along the x-axis and

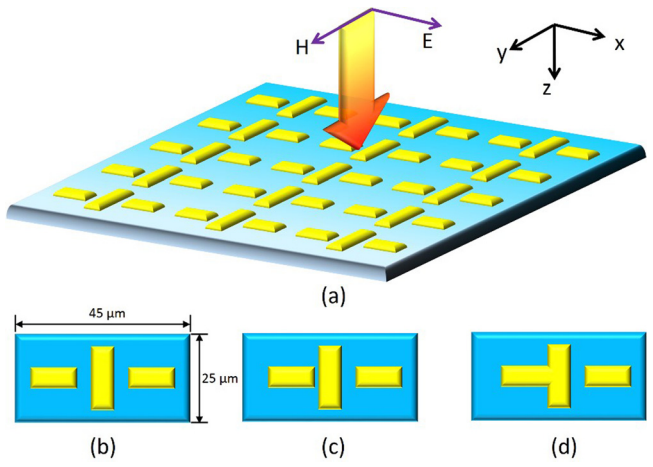

FIG. 1. Schematic of the reconfigurable metamaterial: (a) perspective review; (b) metamolecule before L-strip shifting; (c) metamolecule after the L-strip shifts and breaks the metamolecule symmetry; (d) L-strip in contact with the C-strip.

[a)]W. Zhang and M. Zhang contributed equally to this work.
[b)]Author to whom correspondence should be addressed: wuzhang01@fas.harvard.edu.

located at the two sides of the center strip. The three strips are named the L-strip, the C-strip, and the R-strip when viewed from the left to the center and to the right, respectively. The lattice constant of the metasurface is 45 μm × 25 μm in the xy-plane. The L-strip and the R-strip are 12 μm in length and 6 μm in width. The C-strip is 16 μm in length and 6 μm in width. The gaps between adjacent strips in one metamolecule are 4 μm initially, which makes the metamolecule a symmetric structure as shown in Fig. 1(b). The C-strip and the R-strip are patterned on a bulk substrate, while the L-strip is on a suspended beam and can be moved along the x-direction through a micromachined actuator. Therefore, the gap between the L-strip and the C-strip can be changed during the L-strip movement. The symmetric state of the metamolecule is then broken, and the L-strip continues to move until it comes into contact with the C-strip as illustrated in Figs. 1(c) and 1(d), respectively. Couplings between the strips are changed, and the THz response of the metasurface is tuned.

First, we analyzed the THz response from the metamaterial only consisting of the L-strip and the R-strip. The transmission spectra under x-polarized THz wave incidence are numerically analyzed by using Microwave Studio of Computer Simulation Technology (CST) in the periodic boundary condition. The gap between the L-strip and the R-strip is noted as g_0 as shown in Fig. 2. With a small gap of $g_0 = 2\,\mu$m, a strong resonant dip is observed at 2.87 THz. The resonant frequency shifts to 2.88 THz and 2.89 THz when g_0 increases to 4 μm and 8 μm, respectively. As well known, the resonant frequency $f \propto 1/\sqrt{LC}$, where L and C are the effective inductance and the effective capacitance of the metamolecule, respectively. Therefore, the resonant frequency is blue shifted as the capacitance between the L-strip and the R-strip decreases. As g_0 further increases from 14 μm to 20 μm, however, the resonant frequency decreases from 2.89 THz to 2.86 THz. The resonant frequency is red shifted because the coupling between the L-strip in one metamolecule and the R-strip in the next metamolecule begins to dominate. In this periodic structure, the gap between the two strips becomes smaller as g_0 increases and the effective capacitance becomes larger. The Q factor is reduced at a smaller g_0 because the EM wave is easier to be coupled in between the slabs with a smaller gap. To induce a multi-mode resonance, we integrated a different oriented C-strip to the structure with the L-strip and the R-strip. The transmission of the single C-strip is first calculated, and a sharp resonance is observed at 2.88 THz as shown in the red line of Fig. 2, which is in the same resonant regime with the L-strip and R-strip structure.

The C-strip is integrated at the center of the L-strip and the R-strip. The gaps between the strips in one metamolecule are the same and are noted as g_1. The transmission spectra of the structure are calculated as shown in Fig. 3(a). Only one resonance is induced in the symmetric structure with different g_1 values. However, unlike the resonance shifting in Fig. 2, the resonance in the symmetric three-strip structure is fixed at 2.87 THz when g_1 increases from 1 μm to 5 μm and slightly shifted to 2.86 THz when g_1 further increases to 6 μm. It is also noticed that the Q factor of the resonance becomes larger when g_1 increases from 1 μm to 3 μm and then gets smaller when g_1 further increases from 4 μm to 6 μm. To understand the gap dependence of the resonant

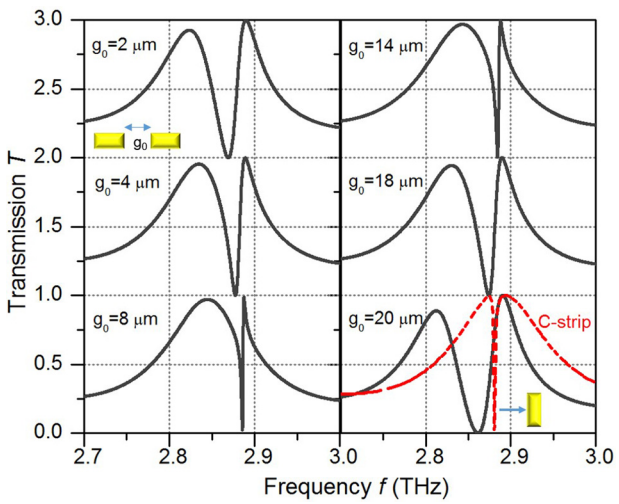

FIG. 2. Calculated transmission spectra of the metamaterial composed of the L-strip and the R-strip with g_0 increasing from 2 μm to 20 μm (black solid line) and the spectrum of the metamaterial composed of the C-strip (red dashed line).

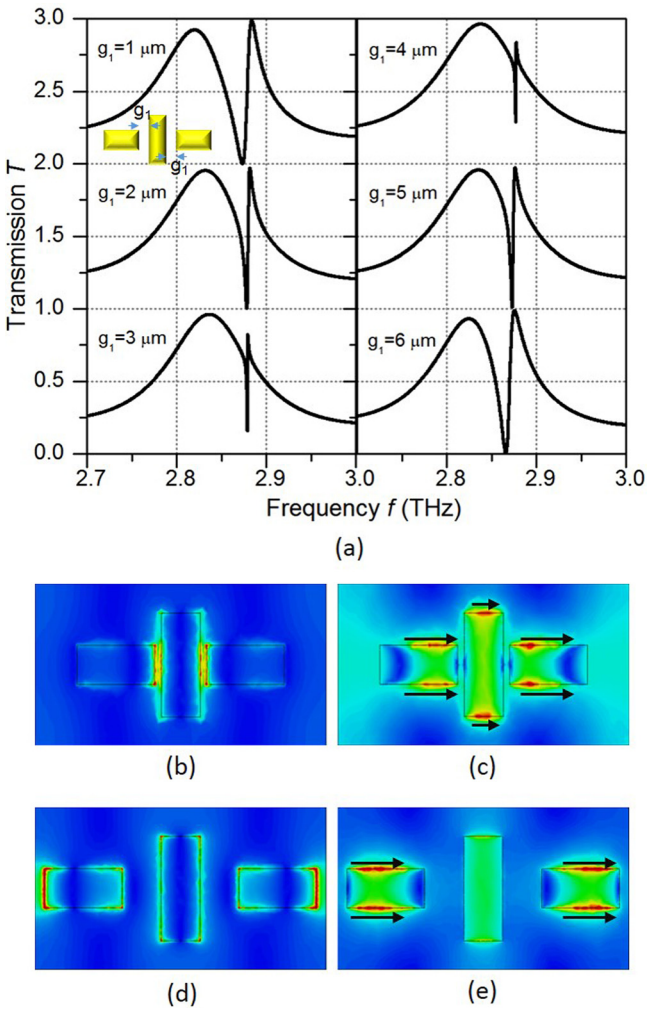

FIG. 3. (a) Calculated transmission spectra with g1 increasing from 1 μm to 6 μm; (b) electric field and (c) magnetic field at 2.87 THz of the metamolecule when the L-strip moved with $g_1 = 1\,\mu$m; (d) electric field and (e) magnetic field at 2.86 THz of the metamolecule when the L-strip moved with $g_1 = 6\,\mu$m. The black arrow indicates the surface current flow direction.

frequency, the induced electric field and magnetic field on the metamaterial are investigated and compared for $g_1 = 1\ \mu$m at 2.87 THz [Figs. 3(b) and 3(c)] and $g_1 = 6\ \mu$m at 2.86 THz [Figs. 3(d) and 3(e)], respectively. The field intensity is indicated using the color map. Strong electric field coupling is observed between the strips at the resonant frequency of 2.87 THz when $g_1 = 1\ \mu$m. Large surface currents, indicated by the black arrow, are induced on the three strips and flow in the same direction. Therefore, the resonant dip is due to the total coupling effect of the three strips. When $g_1 = 6\ \mu$m, the electric coupling between the L (or R)-strip and the C-strip decreases. However, the coupling between the L (or R) strip in one metamolecule and the R (or L)-strip in the next metamolecule increases. Meanwhile, the surface current on the C-strip deceases significantly, which indicates that the resonance depends mainly on the current oscillation on the L-strip and the R-strip.

We then change the gap between the L-strip and the C-strip while fixed that between the R-strip and C-strip to induce asymmetric couplings in the two gaps. Initially, the gaps at both the left side and the right side are 4 μm. The left side gap, noted as g_2, then decreases from 4 μm to 0 by moving the L-strip to the positive x-direction until coming into contact with the C-strip. The transmission spectra during the movement are calculated as shown in Fig. 4(a). Initially, a single resonance is observed at 2.87 THz. When g_2 is decreased to 2 μm, a new resonance at 2.84 THz is excited, while the resonance at 2.87 THz remains the same. The new resonance gets stronger and shifts to 2.83 THz when g_2 is further decreased to 1 μm. The transmission spectrum is changed significantly when g_2 becomes 0, and only one resonance at 2.87 THz is excited. In this condition, the L-strip comes into contact with the C-strip, the capacitive coupling between them is vanished, and the electrons can directly flow between the two strips.

The electric and magnetic fields at the resonances of 2.84 THz when $g_2 = 1\ \mu$m [Figs. 4(b) and 4(c)] and 2.87 THz when $g_2 = 0$ [Figs. 4(d) and 4(e)] are investigated. When $g_2 = 1\ \mu$m, strong electric couplings are induced between the L-strip and the C-strip, while almost no coupling is observed between the R-strip and the C-strip as indicated by the calculated electric field. It is also noted that the surface current on the L-strip and the R-strip flows in opposite directions, which is due to the asymmetric coupling with the C-strip. As g_2 becomes 0 and the L-strip comes into contact with the C-strip, the capacitive coupling only exists between the C-strip and the R-strip. The surface current concentrates on the R-strip and the contacted corners in L- and C-strips. The current flows in the same direction and is due to the capacitive coupling. Therefore, during the movement of the L-strip, a single mode resonance is tuned to a dual mode resonance by breaking the symmetry of the capacitive coupling and is tuned to one mode again when one side capacitance is shorted.

The tunable asymmetric coupling is demonstrated by a micromachined fabricated RMM. The SEM graph of the RMM is shown in Fig. 5(a). Metallic strips are fabricated by patterning a 500-nm-thick aluminum layer on a SOI (silicon on insulator) substrate through optical lithography processes. The L-strip is isolated with the other two by etching a gap

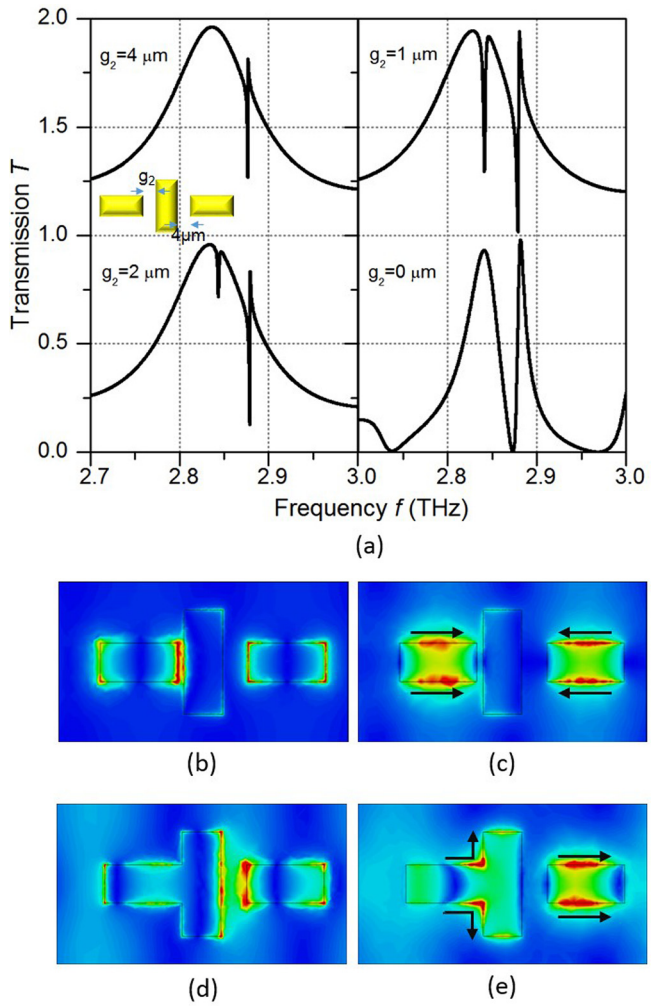

FIG. 4. (a) Calculated transmission spectra with g_2 decreasing from 4 μm to 0; (b) electric field and (c) magnetic field of the metamolecule at 2.84 THz when the L-strip moved with $g_2 = 1\ \mu$m; (d) electric field and (e) magnetic field of the metamolecule at 2.87 THz when the L-strip moved with $g_2 = 0$. The black arrow indicates the surface current flow direction.

between them through the deep reactive ion etching process. The oxide layer under the L-strip is then released from the substrate by HF vapor, and the L-strip becomes movable. The movement is fulfilled through an electrical voltage controlled micromachined actuator. In the initial state, both the gap between the L-strip and the C-strip and the gap between the R-strip and the C-strip are 4 μm. The L-strip is moved to the right side and comes into contact with the C-strip with a total displacement of 4 μm with an electric bias of 10 V.

The transmission spectra of the RMM are measured using FTIR in different L-strip moving states as shown in Fig. 5(b). When g_2 is 4 μm, the strips are in the symmetric structure and a resonant dip at 2.99 THz is induced. A weak resonance at 2.94 THz is also observed. This resonance comes from the asymmetric of the substrate, which is a suspended beam under the L-strip, while a bulk solid under the C-strip and the R-strip. When the L-strip moves to the right side and g_2 decreases to 2 μm and 1 μm, due to the stronger coupling between the L-strip and the C-strip, the resonance at 2.99 THz remains the same, while the resonant dip at 2.94 THz becomes deeper. When the two strips come into contact, the transmission spectra change significantly with a

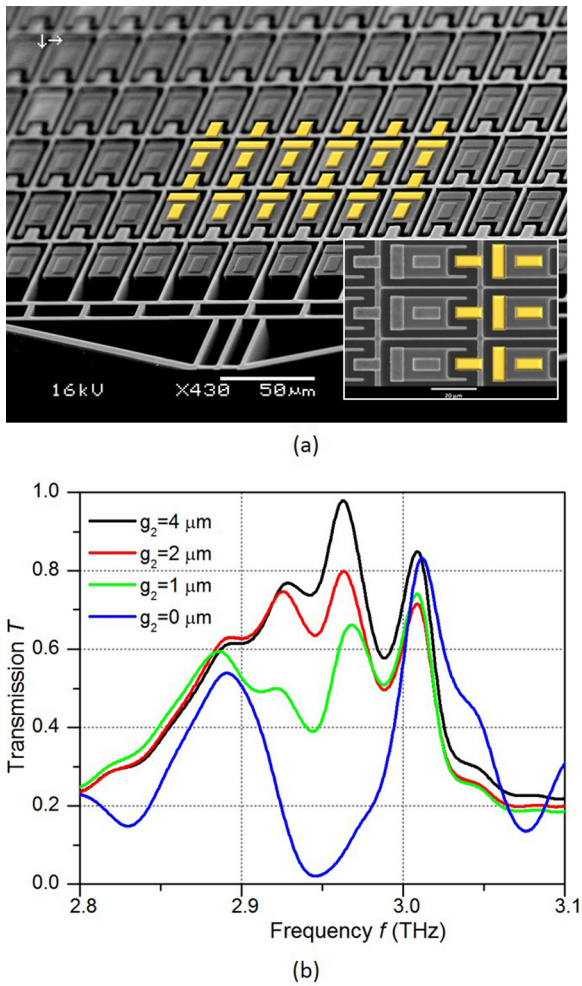

FIG. 5. (a) SEM graph of the reconfigurable metamaterial (inset: metamolecules of the metamaterial); (b) measured transmission spectra at different g_2 values.

large resonance at 2.94 THz induced, which stems from the coupling between the R-strip and the contacted two strips.

In conclusion, we discussed the tunability in a RMM by changing the coupling between metallic strips in the metamolecule. The resonant frequency shifting and the Q-factor of the resonance are effectively manipulated through the coupling change. A switching between a single resonance and a dual resonance in the THz regime is demonstrated by breaking the symmetric of the metamaterial. The switchable metamaterial can be widely applied as optical switches, filters, and THz detectors.

[1]R. M. Walser, "Electromagnetic metamaterials," Proc. SPIE **4467**, 1–15 (2001).
[2]R. Marqués, J. Martel, F. Mesa, and F. Medina, "A new 2D isotropic left-handed metamaterial design: Theory and experiment," Microwave Opt. Technol. Lett. **35**, 405–408 (2002).
[3]M. Chen, X. Xiao, L. Chang, C. Wang, and D. Zhao, "High-efficiency and multi-frequency polarization converters based on graphene metasurface with twisting double L-shaped unit structure array," Opt. Commun. **394**, 50–55 (2017).
[4]D. R. Smith, W. J. Padilla, D. C. Vier, S. C. Nemat-Nasser, and S. Schultz, "Composite medium with simultaneously negative permeability and permittivity," Phys. Rev. Lett. **84**, 4184–4187 (2000).
[5]S. Linden, C. Enkrich, M. Wegener, J. Zhou, T. Koschny, and C. M. Soukoulis, "Magnetic response of metamaterials at 100 terahertz," Science **306**, 1351–1353 (2004).
[6]J. Valentine, S. Zhang, T. Zentgraf, E. Ulin-Avila, D. A. Genov, G. Bartal, and X. Zhang, "Three-dimensional optical metamaterial with a negative refractive index," Nature **455**, 376–379 (2008).
[7]M. Kafesaki, I. Tsiapa, N. Katsarakis, T. Koschny, C. M. Soukoulis, and E. N. Economou, "Left-handed metamaterials: The fishnet structure and its variations," Phys. Rev. B **75**, 235114 (2007).
[8]T. F. Gundogdu, N. Katsarakis, M. Kafesaki, R. S. Penciu, G. Konstantinidis, A. Kostopoulos, E. N. Economou, and C. M. Soukoulis, "Negative index short-slab pair and continuous wires metamaterials in the far infrared regime," Opt. Express **16**, 9173–9180 (2008).
[9]R. A. Shelby, D. R. Smith, and S. Schultz, "Experimental verification of a negative index of refraction," Science **292**, 77–79 (2001).
[10]V. M. Shalaev, "Optical negative-index metamaterials," Nat. Photonics **1**, 41–48 (2007).
[11]B. Luk'Yanchuk, N. I. Zheludev, S. A. Maier, N. J. Halas, P. Nordlander, H. Giessen, and C. T. Chong, "The Fano resonance in plasmonic nanostructures and metamaterials," Nat. Mater. **9**, 707–715 (2010).
[12]S. Zhang, D. A. Genov, Y. Wang, M. Liu, and X. Zhang, "Plasmon-induced transparency in metamaterials," Phys. Rev. Lett. **101**, 047401 (2008).
[13]N. Liu, L. Langguth, T. Weiss, J. Kästel, M. Fleischhauer, T. Pfau, and H. Giessen, "Plasmonic analogue of electromagnetically induced transparency at the Drude damping limit," Nat. Mater. **8**, 758–762 (2009).
[14]A. V. Kildishev, A. Boltasseva, and V. M. Shalaev, "Planar photonics with metasurfaces," Science **339**, 1232009 (2013).
[15]D. Lin, P. Fan, E. Hasman, and M. L. Brongersma, "Dielectric gradient metasurface optical elements," Science **345**, 298–302 (2014).
[16]D. Schurig, J. J. Mock, B. J. Justice, S. A. Cummer, J. B. Pendry, A. F. Starr, and D. R. Smith, "Metamaterial electromagnetic cloak at microwave frequencies," Science **314**, 977–980 (2006).
[17]W. Cai, U. K. Chettiar, A. V. Kildishev, and V. M. Shalaev, "Optical cloaking with metamaterials," Nat. Photonics **1**, 224–227 (2007).
[18]J. Valentine, J. Li, T. Zentgraf, G. Bartal, and X. Zhang, "An optical cloak made of dielectrics," Nat. Mater. **8**, 568–571 (2009).
[19]X. Zhang and Z. Liu, "Superlenses to overcome the diffraction limit," Nat. Mater. **7**, 435–441 (2008).
[20]N. I. Landy, S. Sajuyigbe, J. J. Mock, D. R. Smith, and W. J. Padilla, "Perfect metamaterial absorber," Phys. Rev. Lett. **100**, 207402 (2008).
[21]K. Aydin, V. E. Ferry, R. M. Briggs, and H. A. Atwater, "Broadband polarization-independent resonant light absorption using ultrathin plasmonic super absorbers," Nat. Commun. **2**, 517 (2011).
[22]X. Liu, T. Starr, A. F. Starr, and W. J. Padilla, "Infrared spatial and frequency selective metamaterial with near-unity absorbance," Phys. Rev. Lett. **104**, 207403 (2010).
[23]F. Aieta, P. Genevet, M. A. Kats, N. Yu, R. Blanchard, Z. Gaburro, and F. Capasso, "Aberration-free ultrathin flat lenses and axicons at telecom wavelengths based on plasmonic metasurfaces," Nano Lett. **12**, 4932–4936 (2012).
[24]M. Khorasaninejad, W. T. Chen, R. C. Devlin, J. Oh, A. Y. Zhu, and F. Capasso, "Metalenses at visible wavelengths: Diffraction-limited focusing and subwavelength resolution imaging," Science **352**, 1190–1194 (2016).
[25]H. G. Teo, A. Q. Liu, J. Singh, M. B. Yu, and T. Bourouina, "Design and simulation of MEMS optical switch using photonic bandgap crystal," Microsyst. Technol. **10**, 400–406 (2004).
[26]Q. Chang, Q. Li, Z. Zhang, M. Qiu, T. Ye, and Y. Su, "A tunable broadband photonic RF phase shifter based on a silicon microring resonator," IEEE Photonics Technol. Lett. **21**, 60–62 (2009).
[27]C. M. Watts, D. Shrekenhamer, J. Montoya, G. Lipworth, J. Hunt, T. Sleasman, S. Krishna, D. R. Smith, and W. J. Padilla, "Terahertz compressive imaging with metamaterial spatial light modulators," Nat. Photonics **8**, 605–609 (2014).
[28]Z. L. Sámson, K. F. MacDonald, F. De Angelis, B. Gholipour, K. Knight, C. C. Huang, E. Di Fabrizio, D. W. Hewak, and N. I. Zheludev, "Metamaterial electro-optic switch of nanoscale thickness," Appl. Phys. Lett. **96**, 143105 (2010).
[29]N. H. Shen, M. Massaouti, M. Gokkavas, J. M. Manceau, E. Ozbay, M. Kafesaki, T. Koschny, S. Tzortzakis, and C. M. Soukoulis, "Optically implemented broadband blueshift switch in the terahertz regime," Phys. Rev. Lett. **106**, 037403 (2011).
[30]A. Pors and S. I. Bozhevolnyi, "Plasmonic metasurfaces for efficient phase control in reflection," Opt. Express **21**, 27438–27451 (2013).
[31]Y. Zhang, Y. Feng, B. Zhu, J. Zhao, and T. Jiang, "Graphene based tunable metamaterial absorber and polarization modulation in terahertz frequency," Opt. Express **22**, 22743–22752 (2014).

[32]H. T. Chen, W. J. Padilla, J. M. O. Zide, A. C. Gossard, A. J. Taylor, and R. D. Averitt, "Active terahertz metamaterial devices," Nature **444**, 597–600 (2006).
[33]H. T. Chen, W. J. Padilla, M. J. Cich, A. K. Azad, R. D. Averitt, and A. J. Taylor, "A metamaterial solid-state terahertz phase modulator," Nat. Photonics **3**, 148–151 (2009).
[34]H. T. Chen, J. F. O'Hara, A. K. Azad, A. J. Taylor, R. D. Averitt, D. B. Shrekenhamer, and W. J. Padilla, "Experimental demonstration of frequency-agile terahertz metamaterials," Nat. Photonics **2**, 295–298 (2008).
[35]M. Seo, J. Kyoung, H. Park, S. Koo, H. S. Kim, H. Bernien, B. J. Kim, J. H. Choe, Y. H. Ahn, H. T. Kim, N. Park, Q. H. Park, K. Ahn, and D. S. Kim, "Active terahertz nanoantennas based on VO2 phase transition," Nano Lett. **10**, 2064–2068 (2010).
[36]C. Zaichun, M. Rahmani, G. Yandong, C. T. Chong, and H. Minghui, "Realization of variable three-dimensional terahertz metamaterial tubes for passive resonance tunability," Adv. Mater. **24**, OP143–OP147 (2012).
[37]J. Li, C. M. Shah, W. Withayachumnankul, B. S. Y. Ung, A. Mitchell, S. Sriram, M. Bhaskaran, S. Chang, and D. Abbott, "Mechanically tunable terahertz metamaterials," Appl. Phys. Lett. **102**, 121101 (2013).
[38]B. Ozbey and O. Aktas, "Continuously tunable terahertz metamaterial employing magnetically actuated cantilevers," Opt. Express **19**, 5741–5752 (2011).
[39]W. Zhang, A. Q. Liu, W. M. Zhu, E. P. Li, H. Tanoto, Q. Y. Wu, J. H. Teng, X. H. Zhang, M. L. J. Tsai, G. Q. Lo, and D. L. Kwong, "Micromachined switchable metamaterial with dual resonance," Appl. Phys. Lett. **101**, 151902 (2012).
[40]W. M. Zhu, A. Q. Liu, T. Bourouina, D. P. Tsai, J. H. Teng, X. H. Zhang, G. Q. Lo, D. L. Kwong, and N. I. Zheludev, "Microelectromechanical Maltese-cross metamaterial with tunable terahertz anisotropy," Nat. Commun. **3**, 1274 (2012).
[41]M. Zhang, W. Zhang, A. Q. Liu, F. C. Li, and C. F. Lan, "Tunable polarization conversion and rotation based on a reconfigurable metasurface," Sci. Rep. **7**, 12068 (2017).